Cement & Concrete Composites 33 (2011) 179–191

Contents lists available at ScienceDirect

Cement & Concrete Composites

journal homepage: www.elsevier.com/locate/cemconcomp

Micro-analysis of "salt weathering" on cement paste

Zanqun Liu [a,b,c,*], Dehua Deng [a,c], Geert De Schutter [b], Zhiwu Yu [a,c]

[a] School of Civil Engineering and Architecture, Central South University, Changsha, Hunan 410075, PR China
[b] Magnel Laboratory for Concrete Research, Department of Structural Engineering, Ghent University, Ghent 9052, Belgium
[c] National Engineering Laboratory for High Speed Railway Construction, Changsha, Hunan 410075, PR China

ARTICLE INFO

Article history:
Received 22 January 2010
Received in revised form 14 October 2010
Accepted 15 October 2010
Available online 23 October 2010

Keywords:
Micro-analysis
Salt weathering
Cement paste
Sulfate attack

ABSTRACT

Normally, concrete technologists attribute salt weathering, salt crystallization or physical attack to the deterioration of concrete that is partially exposed to sulfate environment. However, there are few convincing evidences supporting this view. The purpose of this paper is to check by means of extensive micro-analysis if traces of sulfate crystals are present in the paste. This would enable to verify in a direct way whether salt weathering really causes cement paste damage or not.

In this research, cement paste and cement–fly ash paste specimens were partially exposed to sodium sulfate and magnesium sulfates solution under a constant storage condition (20 ± 2 °C, and 60 ± 5% RH) and a sharply fluctuating environment (40 ± 2 °C and 35 ± 5% RH for 24 h, then 10 ± 1 °C and 85 ± 5% RH, also for 24 h) respectively. ESEM and SEM images, combined with EDS and XRD analysis, were employed for micro-analysis. The experimental results indicate that Na_2SO_4 crystals or $MgSO_4$ crystals could not be identified in the cement paste or the cement–fly ash paste, both under constant and fluctuating exposure conditions. Instead, large amounts of ettringite, gypsum and brucite were found and identified as probably one of the determining factors causing failure of cement paste. On the other hand, salt crystallization could be observed in the calcium carbonate crystals, the carbonated products of hydrated cement paste.

1. Introduction

Salt weathering is one of the most important degradation mechanisms that porous materials, such as stone and masonry, undergo at and near the earth's surface [1]. Salt weathering can result in the failure of the porous material when partially subjected to a salt containing environment, especially with sulfates. Essentially, the salt weathering is salt crystallization in pores. When the porous material is in contact with the soil, salt containing ground water can enter the pores through capillary sorption. The evaporation will lead to an increase of salt concentration in the pore liquid near the dry surface of the porous material in contact with relatively dry air. Salt crystallization occurs in liquids with a high salt concentration and causes the failure of the porous material. The parts of porous materials (stone and rock) in contact with relatively dry air near the earth's surface can be severely deteriorated, but the parts buried in salt environment look sound. A similar phenomenon can be found in concrete elements partially exposed to sulfate environments. Researchers attribute the failure of concrete to salt weathering or salt crystallization [2–8].

However, in case of salt weathering on concrete elements, it has been hard to identify sulfate crystals. This is often attributed to the coring and sawing operations when preparing samples for experimental analysis, as lapping water can readily dissolve salts from original and treated surfaces [2,3,8]. However this is not the main cause for the problem. Samples also can be taken in a dry manner to avoid the influence of water. Furthermore, some long-term field tests and laboratory studies on salt weathering on concrete showed contradictory results compared to salt weathering on stone or rock.

1.1. Long-time field exposure

Since 1940, a long-term study on sulfate attack on concrete was carried out by the Portland Cement Association (PCA) [9–11]. Thousands of concrete beams (152 × 152 × 762 mm) were placed horizontally at a depth of 75 mm in sulfate rich soils (about 5.6% sulfate ion by weight of soil) in Sacramento, California. Per year they were subjected to 10–12 wetting and drying cycles. Other field experiments with concrete cylinders were performed by Irassar [12]. These tests showed the following common appearances:

(1) The parts of the beams above ground, regardless their cement content, cement composition, mineral additions, surface treatments and type of coarse aggregates, were

* Corresponding author at: School of Civil Engineering and Architecture, Central South University, Changsha, Hunan 410075, PR China. Tel./fax: +86 731 82656611.
E-mail address: liuzanqun_2001@hotmail.com (Z. Liu).

0958-9465/$ - see front matter © 2010 Elsevier Ltd. All rights reserved.
doi:10.1016/j.cemconcomp.2010.10.010

severely deteriorated. The parts of the beams under ground, however, showed little or no deterioration;
(2) Pozzolanic additions, such as fly ash, furnace slag or silica fume, play a negative role in the performance of concrete exposed to these conditions;
(3) The water-to-cementitious material ratio (W/CM) is the primary factor affecting the durability and performance of concrete in contact with sulfate soils: applying a low W/CM ratio results in a higher resistance to sulfate attack;
(4) The cement type (Type I, Type II and Type V) and type of mineral addition used are the most important parameters with respect to sulfate resistance of concrete.

Concerning the deterioration mechanism, researchers attributed the failure of concrete to physical attack or salt crystallization. However, two conflicting conclusions can be drawn from the abovementioned field experiments:

(1) Role of binder type. For different concretes with comparable strength and pore structure, salt crystallization damage is expected to be comparable. However, it was found that a mere change of cement type significantly changed the resistance of the concrete to the given exposure conditions. When adding pozzolan additions, a more severe degradation was observed. Irassar [12] attributed this to a refinement of pores due to these mineral additions, as the pore size refinement contributes to an increase in capillary suction height. However, this is in conflict with the following observations.
(2) Role of water-to-cement ratio (W/C). Following the explanation based on the height of capillary sorption, concrete with a low W/C ratio should be more susceptible to salt weathering than with high W/C ratio. In the paper by Nehdi and Hayek [13], we can find that the sorption height of mortar with W/C of 0.45 is higher than with W/C of 0.6. If the above explanation is right, the mortar with low W/C (0.45) should be more susceptible to damage than the mortar with high W/C (0.6). Obviously, this reasoning leads to a contradiction.
(3) In effect, according to the XRD, optical microscopy and SEM analysis done by Stark, a large amount of chemical sulfate attack products, such as ettringite, gypsum and thaumasite, were identified in the upper part of concrete in contact with air. However, the samples for these tests were drilled with water [11].

Based on the results of the long-term field exposure tests, we cannot conclude with certainty that salt crystallization is causing the concrete damage. The outcome of some laboratory experiments also cannot be explained by salt crystallization.

1.2. Laboratory studies

Rodriguez-Navarro and Doehne [14] studied the effect of evaporation on salt weathering distress on stone. After 30 days of exposure to a saturated sodium sulfate solution at constant 20 °C, larger amounts of efflorescence and lower weight losses were observed when the crystallization took place at a relative humidity of 60% instead of at 30% RH. On the other hand, Haynes et al. partially exposed the same concrete cylinders to 5% Na_2CO_3 and NaCl solutions, respectively [15]. Severe damage was observed for concrete cylinders, which were placed in the constant environment at 20 °C and 54% relative humidity from day 28 to day 530, and then at 20 °C and 32% RH from day 530 to day 1132 (storage condition 1). However, the specimens kept in a constant environment at 20 °C and 54% relative humidity from day 28 to day 1132 (storage condition 2), did not show any damage. These observations can be explained by the fact that a low relative humidity results in more evaporation, leading to sub-efflorescence [16] that forms deep in the material and results in significant damage [17,18].

However, contradictory observations can be found with respect to concrete [19]. Two concrete specimens were partially immersed in the same Na_2SO_4, solution. One specimen was placed at 80% ± 5% RH and the other was placed at 30% ± 5%. After 75 days of exposure to a constant temperature of 25 °C, the specimens at 80% RH showed signs of deterioration first over a very large area, starting from above the solution level. On the contrary, at 30% RH, the zone of deterioration was narrower and was situated at a certain distance above the solution level. In this case, the first sign of deterioration was a crack, not spalling. In another study [8], Haynes compared the performance of concrete specimens partially exposed to the Na_2SO_4 solution, the concrete cylinders and test program being the same as in the abovementioned paper [15]. A completely different visual observation was done: narrower deterioration zones were observed in the concrete cylinders, which were exposed to exposure condition 1, and extensive spalling was found in case of specimens exposed to exposure condition 2. Abundant gypsum deposits were found in large and small cracks and micro-cracks. Voids were also observed on the outer concrete surface. These experimental results show that higher relative humidity conditions (low evaporation rate) cause a more severe deterioration of the concrete when exposed to sulfates. These findings are not in correspondence with the basic mechanisms of salt crystallization.

1.3. Purpose of this study

Given these contradictions, it is not convincing to attribute the failure of concrete elements exposed to sulfates to salt weathering or salt crystallization. Others factors must play an important role. To make sure whether it is the salt crystallization that causes the failure of porous materials, the direct approach is to identify whether there are some traces of sulfate crystals in the pores. This can be done by means of micro-analysis, such as ESEM combined with EDS and XRD. As to the crystallization in stone or rock, it is common to find thenardite (Na_2SO4), mirabilite ($Na_2SO_4{\cdot}10H_2O$) and epsomite ($MgSO_4{\cdot}7H_2O$) in the pores [20,21]. For concrete elements, these salt crystals were often not identified. This was mainly attributed to the effect of the washing water during sample preparation [2,3,8]. In this paper, we try to detect traces of sulfate crystals in cementitious materials that were not influenced by washing water. The samples prepared for the microscopy tests did not touch water or solution again after removal from the test solution.

Ruiz-Agudo et al. [22] studied salt weathering distress of limestone specimens submerged in a 19.4 g/100 ml sodium sulfate solution and a 33.5 g/100 ml magnesium sulfate solution respectively and located in a controlled environment (20 °C ± 2 °C, and 45% ± 5% RH). Results showed that the limestone specimens were severely damaged in both cases. While salt weathering by sodium sulfate consisted of a detachment of successive stone layers, magnesium sulfate induced the formation and propagation of cracks within the bulk stone. Thenardite and epsomite crystals were identified by ESEM in the pores of limestone. In the present study, similar experiments are performed. The cementitious materials are exposed to sodium sulfate and magnesium sulfate solution respectively in a controlled environment (20 ± 2 °C, and 60 ± 5% RH). According to the diagrams of mirabilite–thenardite conversion under different environmental conditions [8], thenardite (Na_2SO_4) can be formed in the controlled environment.

On the other hand, regarding the distress caused by the crystallization of sodium sulfate, there are two points of view. One school thinks that the crystallization of thenardite is more destructive [23], because the crystallization of thenardite can generate higher

Table 1
Chemical composition of cement and fly ash (% by mass).

	CaO	SiO_2	Fe_2O_3	MgO	Al_2O_3	SO_3	CO_2	Na_2O	K_2O	Ignition loss
Cement	62.21	19.12	3.79	0.86	5.39	3.06	0.72	–	–	1.65
Fly ash	4.46	53.31	7.53	2.45	26.43	0.9	–	1.15	0.9	4.0

pressure than mirabilite at the same supersaturation [24]. Another school points out that the dissolution of thenardite producing a solution highly supersaturated with respect to mirabilite will cause the precipitation of mirabilite and result in the damage of porous materials [25,26].

In the field, temperature and relative humidity (RH) fluctuate significantly, and this absolutely influences the crystallization products of sodium sulfate solution. Thus, it is not sufficient to just study cementitious materials subjected to constant conditions, favoring thenardite formation. Therefore, we also studied the effect of fluctuating environments where transformation between thenardite and mirabilite occurs. According to the study of Rijniers by means of Nuclear Magnetic Resonance (NMR) [27], nucleation of mirabilite is difficult in temperature induced supersaturation experiments. Genkinger and Putnis [28] indicated that nucleation of mirabilite from an evaporating sodium sulfate solution is difficult. In the present study, a cyclic condition of both temperature and relative humidity was investigated. Specimens were placed in an oven at 40 ± 2 °C and 35 ± 5% RH for 24 h. Afterwards the specimens were moved to a fridge at 10 ± 1 °C and 85 ± 5% RH, also for 24 h. In this cyclic process, there is not only abrupt cooling, but also wetting and drying.

In another paper by the authors [29], the performance of concrete partially exposed to sodium and magnesium sulfate solutions was studied by means of ESEM, SEM, EDS and XRD. The experimental results show that concrete damage initiates in the interfacial transition zone due to the formation of ettringite and gypsum. In this paper, we will further focus on the micro-analysis of "salt weathering" on cement paste.

2. Experiments

2.1. Raw materials

In this research, an ordinary Portland cement (CEM I 52.5N), complying with EN 197-1 (2000), and a class F fly ash were used. Table 1 gives the chemical composition of both the cement and fly ash used. A 10% sodium sulfate solution by mass and a 20% magnesium sulfate solution were used.

2.2. Immersion tests

Plain cement paste with a W/C ratio of 0.45 has been exposed to immersion tests, as well as cement–fly ash paste with a cement replacement of 25% by mass. The paste for storage under constant conditions was cast in a mould with size of 20 × 20 × 150 mm. The paste for exposure to fluctuating conditions was cast in 150 × 150 × 150 mm cubic steel moulds. After casting, the specimens were covered with a plastic sheet and cured for 24 h at a constant temperature and relative humidity of 20 (2 °C and 90 ± 5% RH, respectively. Then, the specimens were removed from the moulds and cured in water at 20 ± 1 °C. At the age of 15 days, the cubic specimens were cut into small specimens measuring 10 × 40 × 150 mm. These small specimens were immersed in water again, until the age of 28 days. After 28 days, all specimens were dried in a climate room at 20 ± 2 °C and 60 ± 5% RH for 7 days.

After drying, the specimens for exposure to constant conditions were partially immersed in containers with sodium sulfate solution and magnesium sulfate solution, respectively. The samples were kept in a climate room (20 °C, 60% RH) for a period of 6 months. Fig. 1a shows the setup for the immersion test.

The specimens for exposure to fluctuating environmental conditions were partially immersed in small plastic containers with cover, containing 10% sodium sulfate solution, as shown in Fig. 1b. The depth of the specimen under the solution surface is about 4 cm. The specimens were cyclically placed in an oven for 24 h (40 ± 2 °C, 35 ± 5% RH), and then moved into a fridge for 24 h (10 ± 1 °C, 85 ± 5% RH), as abovementioned.

This test setup simulates the realistic conditions in which foundations and lower parts of walls are exposed to sulfates. The surface of the solution around the specimens was covered, allowing evaporation only through the paste specimens. After immersion, the containers were refilled everyday.

2.3. Visual observation, XRD, SEM, ESEM and EDS analysis

After 5 months of exposure to sulfate solution in a constant environment, the specimens showed signs of deterioration. Under cyclic conditions, the specimens already showed deterioration after three cycles. The damaged specimens were visually observed, and analyzed by means of XRD, SEM, ESEM and EDS. The samples were vacuum dried with silica gel at 20 °C. The specimens did not touch solution and water any more after removal from the solution. The substance on the surface of the specimens was cleaned with a soft brush or a thin blade.

3. Visual observations

3.1. Cement paste exposed to constant condition

3.1.1. Cement paste exposed to sodium sulfate solution

Before immersion, minor shrinkage cracks could be observed in the cement paste specimens, while the cement–fly ash paste specimens did not show visible shrinkage cracks. Benavente [30] pointed out that narrow micro-fissures appear to be important in the decay process due to the effectiveness of crystallization pressure generated by salt growth. So, if crystallization is the mechanism of decay of cement paste, salt crystallization should first occur in the shrinkage cracks and sodium sulfate or

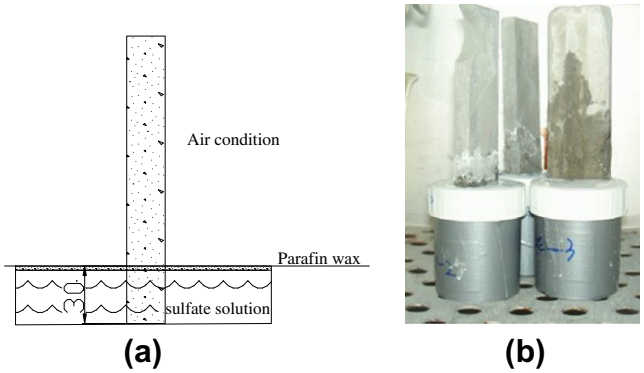

Fig. 1. Schematic of test setup: (a) constant condition and (b) fluctuating condition.

magnesium sulfate crystals should be identified in these cracks. On the other hand, the shrinkage crack is also a weak zone for chemical attack.

Fig. 2 shows the visual appearance of cement paste specimens after 5 months exposure to a 10% sodium sulfate solution. It can be found that: (1) the cement paste specimen is split into several pieces along the shrinkage cracks; (2) on the surface of the crack, two different zones can be distinguished: an inner dark grey zone and an outer white gray zone; (3) white substances are formed at the edge of the surface of outer white grey zone.

Obviously, the products in the outer and inner zone are different. On the other hand, why do white crystals occur on the surface of the outer white grey zone and not on the surface of the inner dark grey zone? What is the white crystal? ESEM, EDS and XRD were used for further analysis.

3.1.2. Cement–fly ash paste exposed to sodium sulfate solution

After 5 months of exposure, the following observations can be made from Fig. 3: (1) compared to the cement paste specimen, the cement–fly ash paste sample was fully covered with white crystals; (2) some cracks were found near the upper edge above solution level of the cement–fly ash paste specimen, while the cement paste specimen looks undamaged. These findings are in correspondence with what was concluded from the abovementioned field exposure tests [9–12]: the upper parts of the concrete beams above ground mixed with pozzolanic additions were deteriorated more severely than the beams made of traditional concrete.

Along the crack, small pieces were carefully broken off using a thin blade (Fig. 3). The products on the surface were identified by means of ESEM, EDS and XRD.

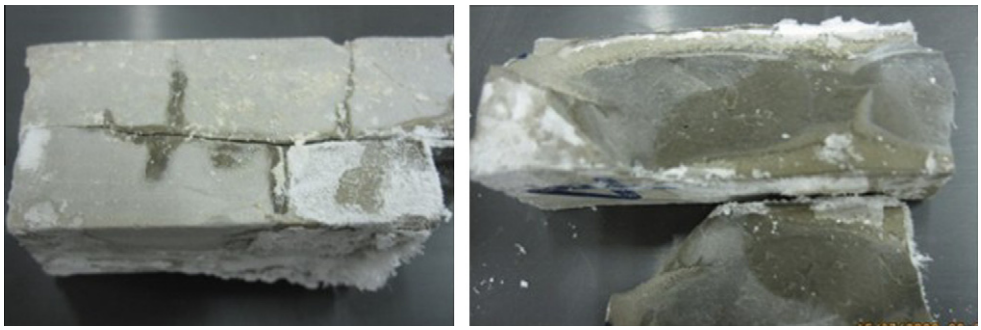

Fig. 2. Visual observation of cement paste specimen exposed to sodium sulfate solution.

Fig. 3. Visual observation of cement–fly ash paste specimen exposed to sodium sulfate solution.

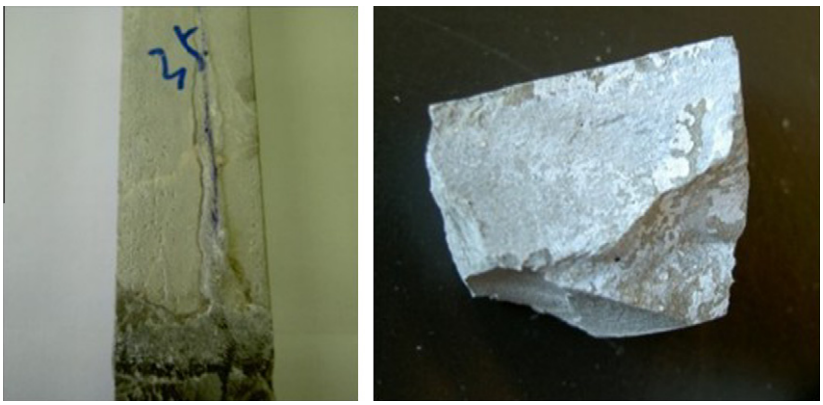

Fig. 4. Visual observation of cement paste specimen exposed to magnesium sulfate solution.

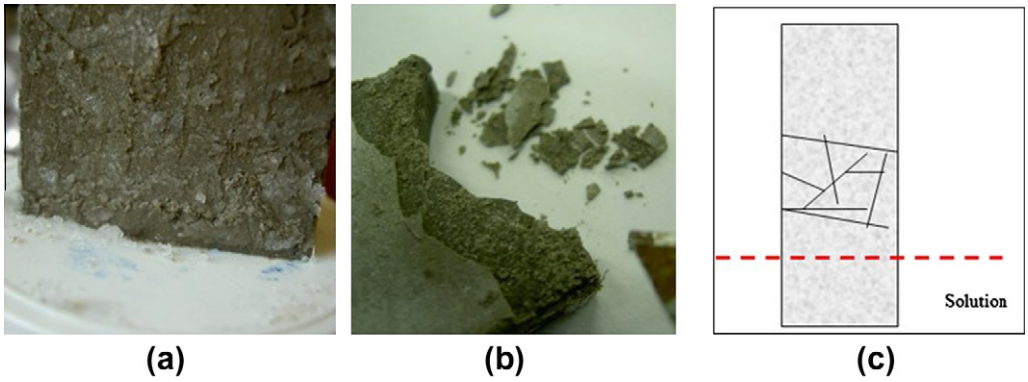

Fig. 5. Visual appearance of specimens after three exposure cycles.

3.1.3. Cement paste exposed to magnesium sulfate solution

Fig. 4 shows the visual appearance of cement paste after 5 months of exposure to a 20% magnesium sulfate solution. One crack covered with a transparent film can be found in the specimen. The specimen was broken easily using a thin blade. A layer of white substance can be observed on the surface of cement paste. The white substance was identified with ESEM and EDS.

3.2. Cement–fly ash paste exposed to fluctuating conditions

Impressively, the cement–fly ash paste specimens exposed to fluctuating conditions were already damaged after three cycles. Fig. 5 shows their visual appearance.

From Fig. 5, it can be noticed there are two kinds of scaling: (1) the specimen was randomly split into several small pieces; (2) an outer layer of paste with thickness (>0.1 mm) was totally detached from the upper part of the paste above the cover of the container (the surface of solution). Fig. 5c schematizes the location of cement paste deterioration. The small pieces broke off along cracks (the black lines). The products on the surface of these small pieces and in the paste were analyzed by means of XRD, SEM and EDS.

4. Micro-analysis and discussion

4.1. Cement paste exposed to constant condition

4.1.1. Cement paste exposed to sodium sulfate solution

As abovementioned, the products on the outer and inner zones and the white substances were identified. Figs. 6–10 show the ESEM, EDS and XRD analysis results. From Fig. 6, it can be found that: (1) the surface of the inner dark grey zone is covered by a large amount of short needle-like crystals, (2) on the right hand side of the image, a cluster of needle-like crystals stretches outwards (in the black circle). The following elements were found in the crystals using EDS: C, Na, Al, Si, S and Ca. There may be several products in the crystals. In order to further identify the products, a layer of powder scraped from the inner dark grey zone was analyzed with XRD. Fig. 7 shows the XRD pattern.

According to this XRD pattern, the main products found are calcium hydroxide, ettringite and calcite. Based on the results of ESEM, EDS and XRD, the main products of the needle crystals should be ettringite and some calcite. Thenardite was not found in the inner dark grey zone.

Fig. 8 shows the ESEM image and EDS analysis of the outer white grey zone. Compared to the inner dark grey zone, the products in the outer white grey zone are relatively simple. A large amount of dense popcorn-like crystals were discovered in this zone. According to the EDS analysis, these crystals should be $CaCO_3$. A layer of powder scraped from the outer white grey zone was also analyzed by means of XRD. Fig. 9 shows the XRD pattern. Compared to Fig. 7, a larger amount of calcite was formed. This means that more of the hydrated cement paste was carbonated. Fig. 10 shows the ESEM image and EDS analysis of the white crystal on the surface of the outer white grey zone. This white crystal was identified as thenardite (Na_2SO_4).

From the micro-analysis on the surface of the shrinkage cracks in the cement paste specimens exposed to sodium sulfate solution, the following conclusions can be drawn: (1) sodium sulfate

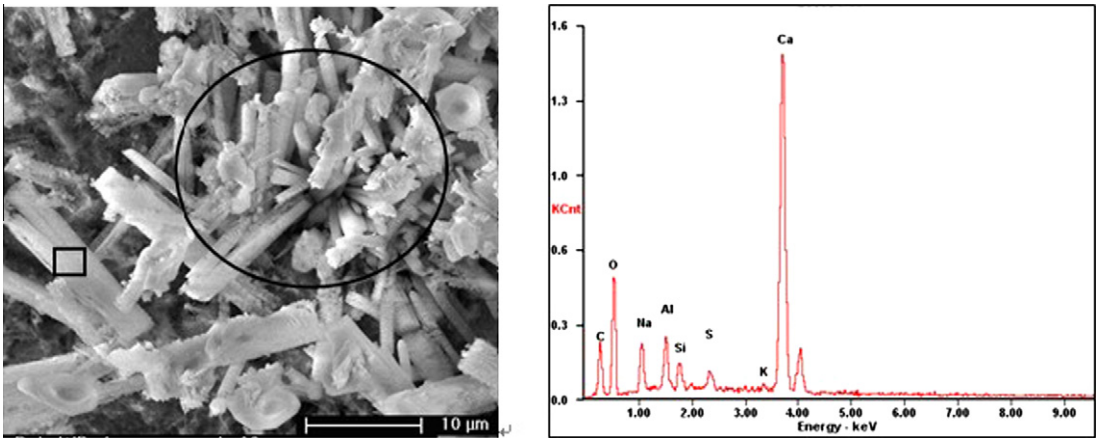

Fig. 6. ESEM and EDS analysis of the products on the surface of inner dark grey zone.

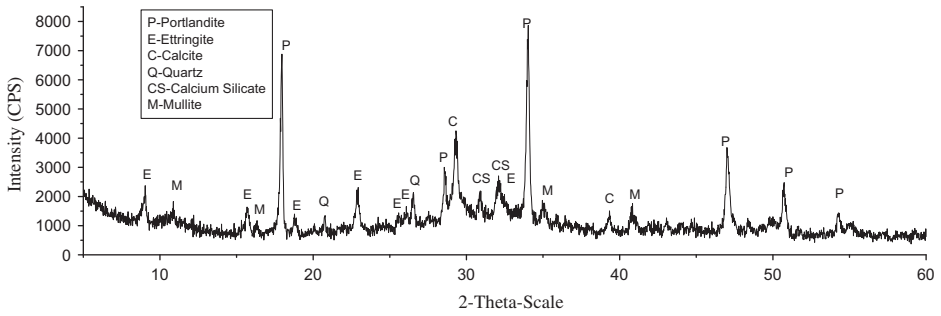

Fig. 7. XRD pattern of the products in the inner dark grey zone of cement paste.

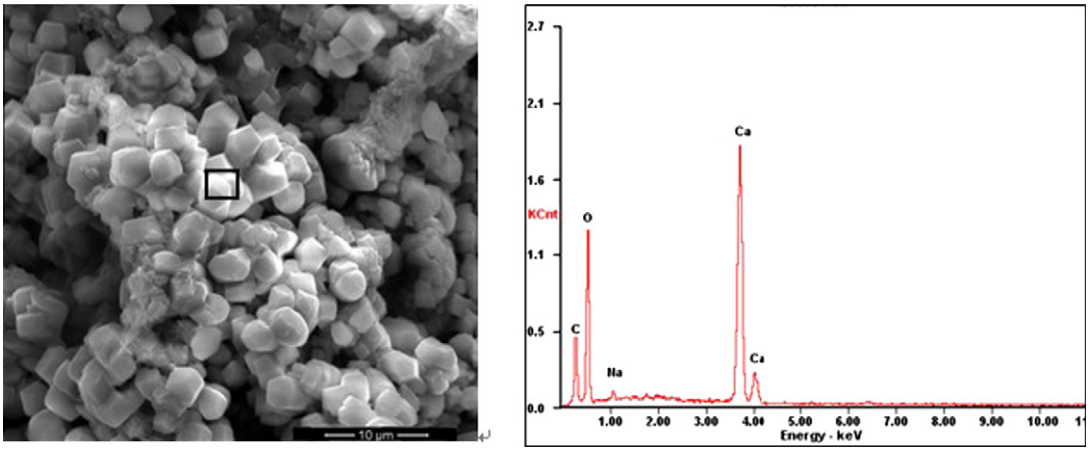

Fig. 8. ESEM and EDS analysis of the products on the surface of outer white grey zone.

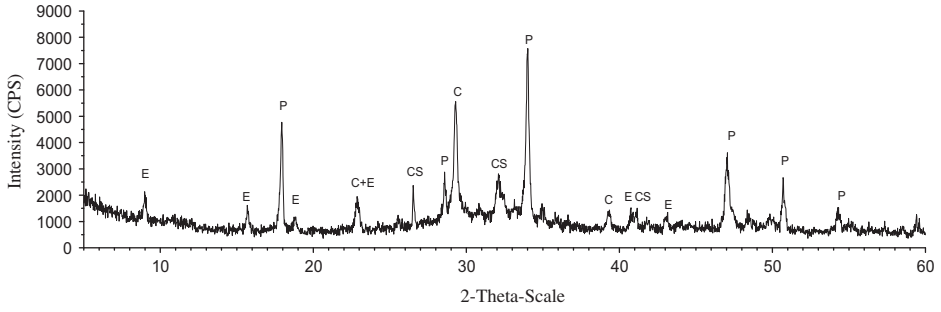

Fig. 9. XRD pattern of the products in the outer white grey part of cement paste.

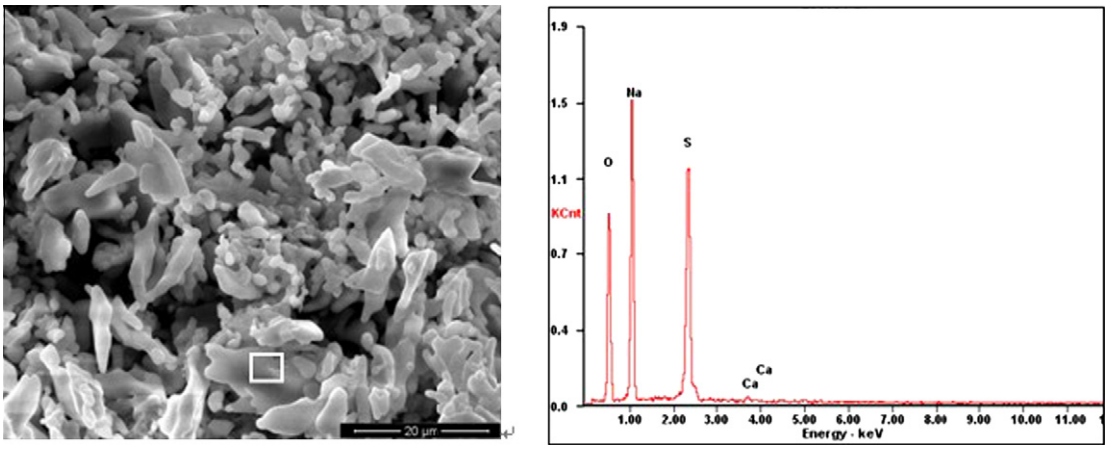

Fig. 10. ESEM and EDS analysis of the white crystal on the surface of the outer zone.

crystals could not be identified in the cement paste; (2) crystallization of sodium sulfate occurred on the surface of the $CaCO_3$ crystals, the carbonated products of hydrated cement paste.

According to the above results, first, it is not likely that sodium sulfate crystallization is responsible for the deterioration of specimens. After the specimen is partially immersed in sodium sulfate solution, the shrinkage cracks will be filled with solution through capillary sorption. In accordance with the mechanism of crystal growth [31], the Na_2SO_4 crystals in the crack will dissolve and diffuse to the surface when in contact with air. As a consequence there is efflorescence and crack covering (on the outer zone of the crack surface in contact with air as shown in Fig. 2). As we know, efflorescence results in little or no damage [17,18].

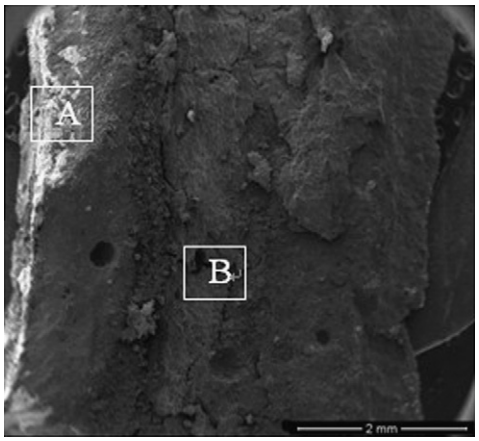

Fig. 11. Section image of small piece.

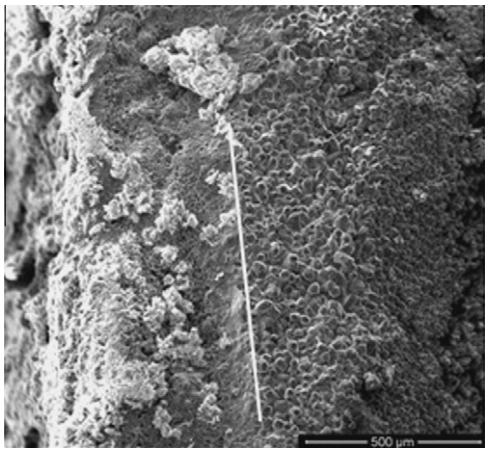

Fig. 12. Zoomed image of zone A.

With respect to ettringite attack, the large crystallization pressures are produced only in small pores (typically < 0.1 μm) [31]. However, fracture is not caused by crystallization in a single pore. It requires crystal growth over a region comparable in size to the strength-controlling flaws [32]. Taylor also pointed out that [33] ettringite crystallization pressure develops in the nanometric pores of the paste, causing an expansion of paste and opening gaps, followed by precipitation of crystals in these gaps. In this case, ettringite crystals first form in the pores and cause expansion. Crystals can easily interact with the shrinkage crack to make them grow and cause the crack to develop, followed by the precipitation of ettringite on the surface of the cracks. In effect, in Fig. 6, we can find a cluster of needle-like crystals stretching outwardly, and the growth of crystals is perpendicular to the surface of crack. Apparently, this will push the paste piece away and cause the crack to develop.

4.1.2. Cement–fly ash paste specimen exposed to sodium sulfate

Fig. 11 shows a zoomed image of Fig. 3 with a magnification of 25 times. The left side is the outer surface in contact with air, and zone A is the surface of a crack. It is necessary to further analyze the products in this zone. As a reference, the products in the inner zone B were also identified. It should be noted that the zone B is a small point in the bulk of the paste.

Fig. 12 shows the zoomed image of zone A. It is interesting to find that two distinct parts can be observed at the right and left hand side of the white line. At the right side a large amount of dense granular crystals cover the surface, while at the left side porous crystals can be found accompanied with white substance. The white substance is thenardite.

From Fig. 13, it can be concluded that the granular crystals are $CaCO_3$. In Fig. 14, according to EDS results, the main elements in the porous crystal area are Ca, O and C, indicating that this is $CaCO_3$ too. However, compared to the granular crystals, the porous crystals are deteriorated. Some crystals are peeled off and crystal caves are left. Some crystals are honeycombed with small pores. According to the EDS analysis, Na and S are also present. Obviously, the crystallization of sodium sulfate results in damage of the $CaCO_3$ crystals.

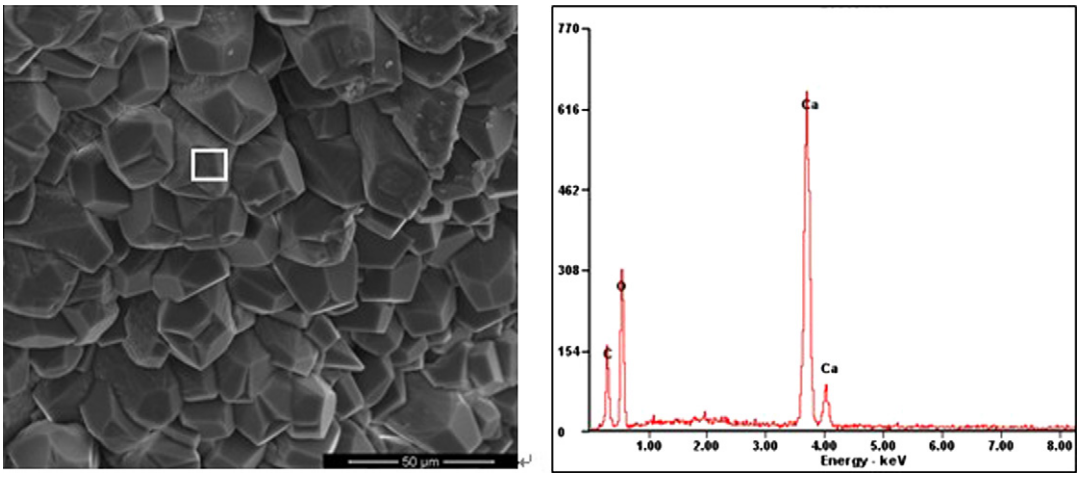

Fig. 13. ESEM image and EDS analysis of *f* the granular crystal in the right part of zone A.

Combining the visual observation and the micro-analysis, it seems that Na_2SO_4 crystallization is not responsible for the crack formation. First, according to the visual observation, the scaling manner in the specimens does not resemble that caused by salt crystallization, similar to that of freezing-and-thawing scaling [8]. Secondly, if salt crystallization would be causing the crack formation, salt crystals should be identified in the right part of zone A (shown in Fig. 12) to form sub-efflorescence instead of in the area in contact with air. Obviously, there should be another phenomenon causing the crack formation.

The crack formation is attributed to some harmful and expansive products present in the paste. As mentioned above, zone B is in the inner zone of the paste. As the small piece was broken off along zone B, this means that zone B is a weak part in the paste. So, zone B could be the source of crack initiation. The analysis of the products in this zone can disclose the real reason that results in the crack formation.

Fig. 15 shows the ESEM and EDS analysis of zone B. A large amount of short needle crystals are found in this zone. According to the EDS analysis, Ca, Al, Si, S, Na, and O elements are present. The crystals are similar to those in the dark grey zone in the shrinkage crack in Fig. 5. XRD was used to further analyze the products. As zone B is in the inner zone of the specimen, the products in this zone should be the same as within the parts of the paste above

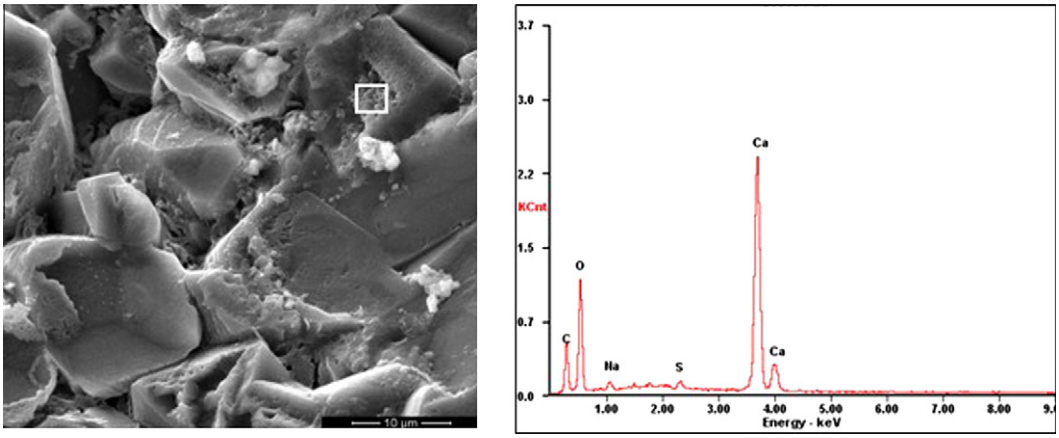

Fig. 14. ESEM image and EDS analysis of the granular crystal in the left part of zone A.

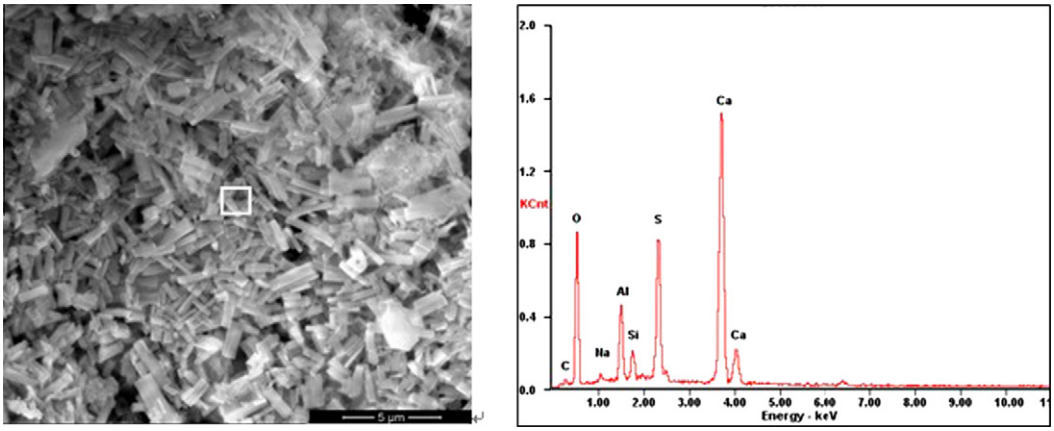

Fig. 15. ESEM and EDS analysis of zone B.

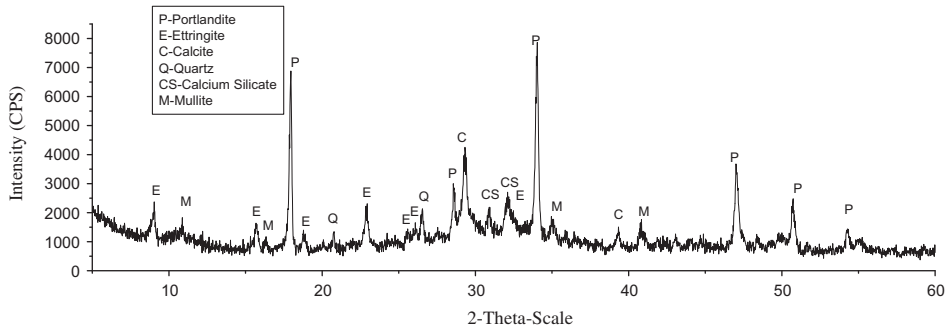

Fig. 16. XRD pattern of upper part of cement–fly ash paste.

solution level where the cracks are formed. Fig. 16 shows the XRD pattern for this area.

As can be seen in the XRD pattern, the main products are calcium hydroxide, calcite, and ettringite. Thenardite was not identified. This supports the idea that the formation of ettringite initiates crack formation in the cement and fly ash paste.

The given experimental results (from Figs. 11–16) help to explain the damage of cement–fly ash paste exposed to sodium sulfate solution. Compared to ordinary cement paste, the cracks in cement–fly ash paste are not shrinkage cracks. They are caused by ettringite formation, the products of chemical sulfate attack. Crystallization of sodium sulfate occurs in $CaCO_3$ crystals. The process of attack can be described as follows: (1) expansive ettringite is first formed, resulting in crack formation; (2) hydrated phases on the surface and in the cracks in contact with air carbonate; (3) salt crystallization occurs in the $CaCO_3$ crystals, causing further deterioration.

Combining the results of Sections 4.1.1 and 4.1.2, apparently, it is very difficult for Na_2SO_4 crystallization to occur in hydrated cement paste. However, it can occur in $CaCO_3$ crystals, the carbonated products of hydrated cement paste. Based on this appearance, an additional test was carried out, as described in another paper [29]. Concrete cylinders with the same mixture proportions were divided into two groups. Before immersion, one group of cylinders was placed in a carbonation chamber (10% CO_2, 20 °C, 60% RH) for 14 days. The other group was not exposed to increased CO_2 levels. Then, the two groups of concrete cylinders were partially exposed to a 5% Na_2SO_4 solution for 8 months. Visual observation shows that the outer layer of carbonation exposed cylinders was severely deteriorated by Na_2SO_4 crystallization. The surfaces of the other cylinders were still sound. These experimental results coincide with the abovementioned observations. It indicates that the Na_2SO_4 crystallization is more likely to occur after concrete carbonation.

4.1.3. Cement paste specimen exposed to magnesium sulfate solution

As shown in Fig. 4, there is a layer of white substance present in the shrinkage crack. Fig. 17 shows the ESEM image of this white crystal.

Two distinct crystals can be distinguished: prismatic crystals surrounded by flocculent crystals. According to the EDS analysis (Figs. 18 and 19), the prismatic crystal is gypsum and the flocculent crystal is brucite. The products of this white substance in the shrinkage cracks are similar to the products in the interfacial zone of concrete fully immersed in magnesium sulfate solution [34]. This supports the statement that the failure of cement paste specimen is caused by chemical sulfate attack.

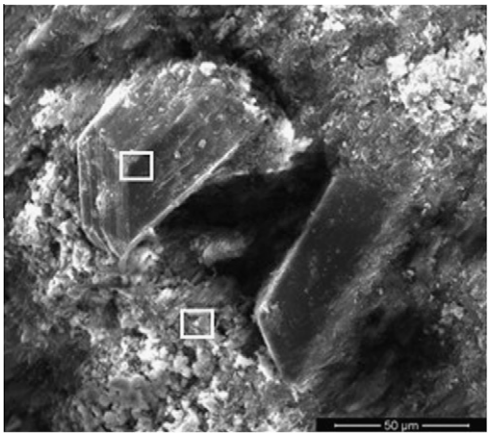

Fig. 17. ESEM image of the white product.

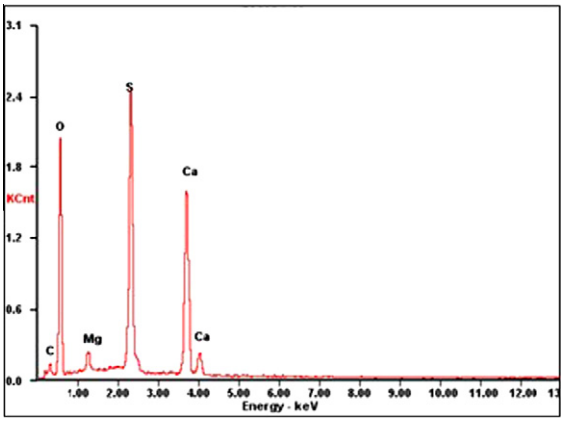

Fig. 18. EDS analysis of prismatic crystal.

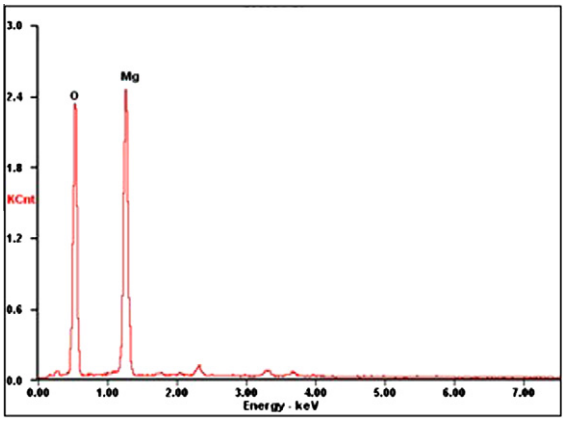

Fig. 19. EDS analysis of flocculent crystals.

4.2. Cement–fly ash paste exposed to fluctuating conditions

With respect to the fluctuating environmental conditions, reaction products were identified on different locations, including: (1) the surface under the outer detached layer; (2) the surface of the cracks.

4.2.1. SEM, EDS and XRD analysis of the products on the surface of cracks

Fig. 20 shows the SEM image and EDS analysis of the surface of a small piece. A large amount of needle-like crystals grow on the surface like a hedgehog. Some pores are filled with a cluster of the needle-like crystals. According to the EDS analysis, the needles are ettringite.

In order to further identify whether sodium sulfate crystals are present in the cement paste, a thin layer of powder on the surfaces of cracks was stripped off and analyzed by means of XRD. Fig. 21 shows the XRD pattern. Ettringite is clearly one of the major products. No Na_2SO_4 crystals were detected.

Wick action is the transport of water (and any substances it may contain) through a concrete (porous materials) surface in contact with water towards a drying face with a relative humidity of less than 100% in the surrounding air [35]. The mechanism involves capillary sorption and evaporation. Capillary forces draw the salty water into the concrete. Evaporation takes place at a wet–dry interface located at a penetration depth near the dry face of the concrete in contact with air after which water vapour diffusion occurs into the dry zone with a relative humidity of less than

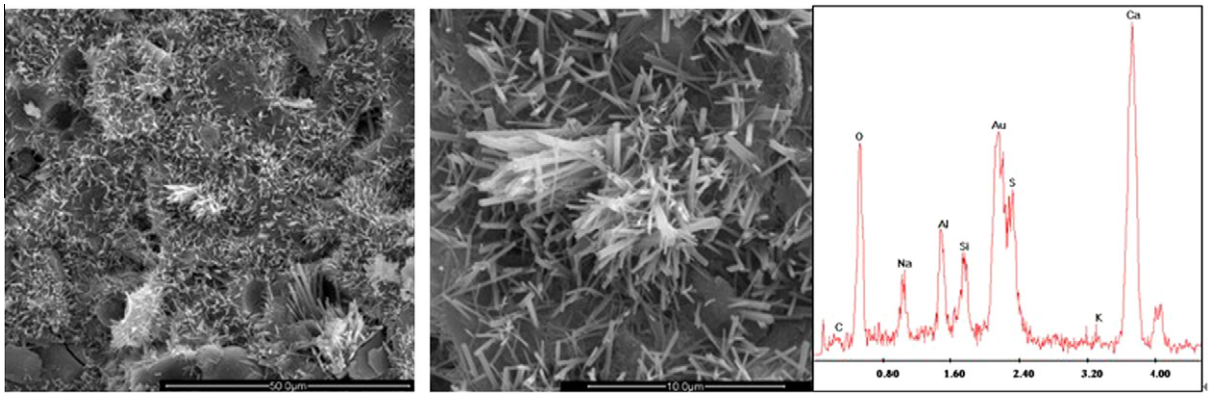

Fig. 20. SEM image and EDS analysis of the surface of internal crack.

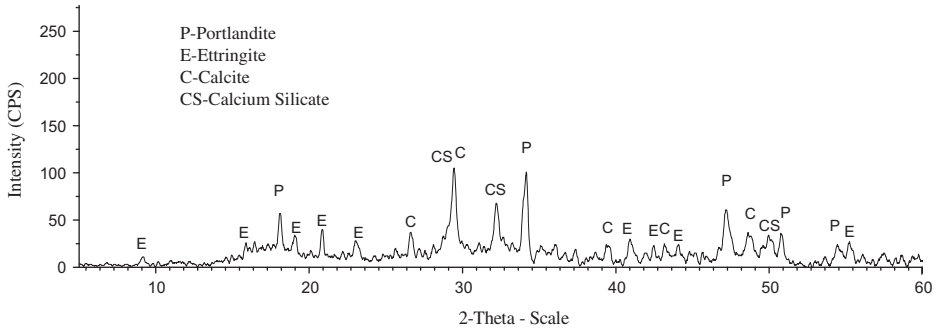

Fig. 21. XRD pattern of the products in the surface powder of visible crack.

100%. After some time, a state of equilibrium (wet–drying interface) may be reached. Then the rate of salt solution entering the concrete by capillary sorption matches the rate of water leaving the opposite face of the concrete element by water vapour diffusion. Salts cannot be carried by vapour and therefore build up at this position. This concentration effect causes back-diffusion of salt away from the wet–dry interface. If the salt concentration near the wet–dry interface ever exceeds the solubility of the salt compounds present, precipitation is likely to occur to form sub-efflorescence [36–39]. The wick action has two consequences. One is that the scaling manner of porous materials is spalled from the surface similar to that of freezing-and-thawing scaling. Another is that an almost saturated Na_2SO_4 pore solution zone is formed in the efflorescence zone of porous materials near the surface of solution [40–42].

In this case, there are two kinds of scaling: a detached layer of paste and several small scaled off pieces (Fig. 5). The small pieces of broken material cannot be the result of salt crystallization. On the other hand, the detached layer of paste seems to be the typical scaling manner for salt crystallization.

According to the results of the abovementioned micro-analysis, ettringite is one of the main products causing scaling of several small pieces after just 6 days. The reason for this phenomenon is the concentration of the pore solution during the wick action process. Based on the analysis above about wick action, different almost saturated sulfate pore solutions will form in the upper part of the paste near the solution level at different temperatures, i.e. at 10 °C the concentration is close to 8 g per 100 g H_2O, and at 40 °C about 45 g per 100 g H_2O [8]. Under severe exposure conditions, ettringite formation is possible in a relative short time. Another reason is that fly ash is activated and forms a large amount of ettringite in a high-concentration Na_2SO_4 solution at high temperature, as shown by thermogravimetric analysis (TGA) [43].

The experimental results of the micro-analysis show again that the formation of ettringite is the determining factor causing the failure of cement–fly ash paste. There is no formation of Na_2SO_4 crystals in the paste even though the fluctuating temperature and relative humidity conditions are favorable for the formation of mirabilite.

4.2.2. SEM, EDS and XRD analysis of the products on the surface of outer detached layer of paste

Compared to the specimens kept under constant exposure conditions, the most visual difference is the presence of an outer layer of paste totally detached from the bulk (Fig. 3). This is in correspondence with sulfate deterioration of limestone. There, a detachment of successive stone layers occurs due to sodium sulfate induced salt weathering distress [22]. Based on these observations it is possible to check whether the paste distress is caused by chemical sulfate attack or salt weathering. Fig. 22 shows the XRD pattern of the outer layer of paste.

From Fig. 22 it can be concluded that the main products of the detached layer of paste are $CaCO_3$ and ettringite. This indicates that the detached layer is almost entirely carbonated. If we could find Na_2SO_4 crystals on the bulk surface under the detached layer, this would mean that Na_2SO_4 crystallization causes the deterioration of outer layer of specimen. Fig. 23 shows the SEM image of this bulk surface.

In the SEM image (a), two main products were detected: the surface is covered by needle-like crystals and some lump – like white substances scattered on the needle-like crystals. Fig. 23b shows the zoomed SEM image of the white substance. It can be observed that a lot of needle-like crystals are molten, resulting in lumpy-like white substances. In the Fig. 23c, the needle-like crystals are almost completely molten, and a piece of relatively pure

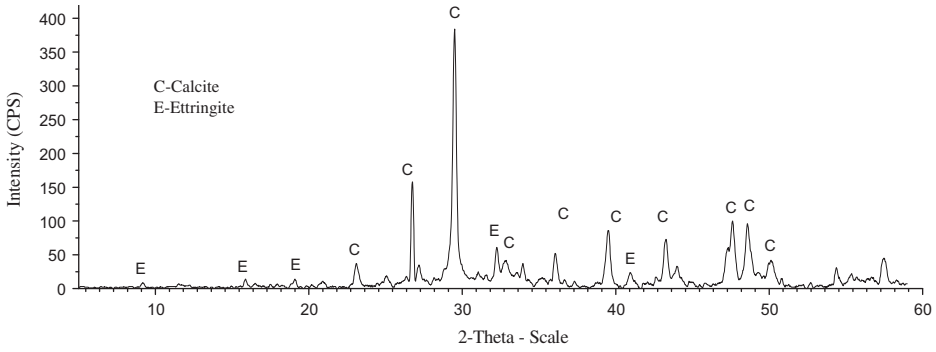

Fig. 22. XRD pattern of the outer layer of paste.

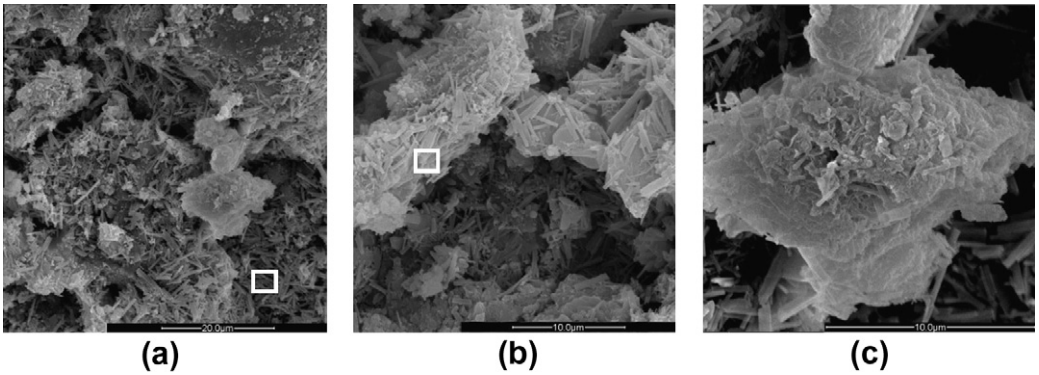

Fig. 23. SEM image of the bulk surface.

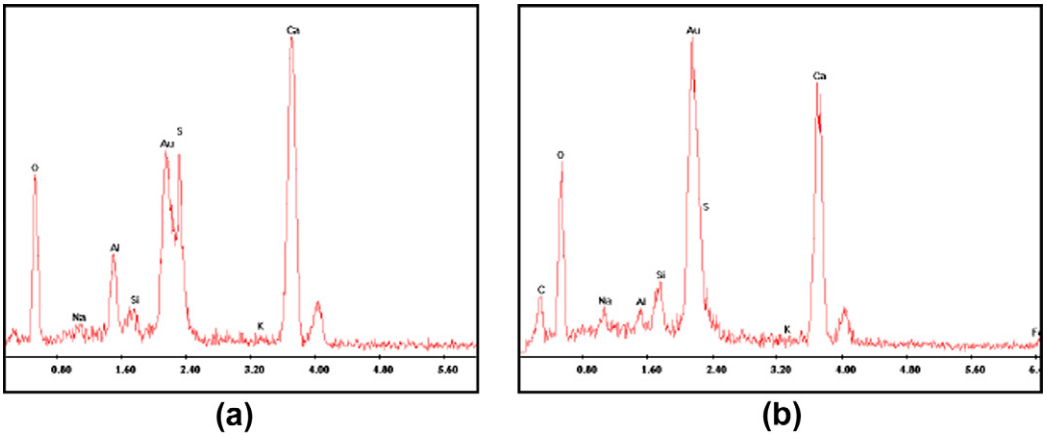

Fig. 24. EDS analysis: (a) the needle-like crystals (Fig. 23a); (b) the white substance (Fig. 23b).

white substance is formed. Fig. 24 shows the EDS analysis of the needle-like crystals (Fig. 23a) and the white substance.

The main elements of the needle-like crystals and the white substance are almost the same, except that also carbon is noticed in Fig. 23b. Based on the XRD analysis of the outer detached layer of paste, the needle-like crystals and the main products of the white surface should be ettringite and $CaCO_3$, respectively.

Apparently, the reason for layer detachment is not salt crystallization but growth of ettringite crystals.

4.2.3. XRD of cement–fly ash paste without the outer detached layer

Fig. 25 shows the XRD pattern of the upper part of paste without the detached layer. Compared to the products on the crack surface (Fig. 21), the main four products in the inner paste are the same, besides the presence of much more portlandite than on the surface. Traces of Na_2SO_4 crystals have not been detected.

4.3. Discussion

In summary, combining the micro-analysis results of previous research [29] and the present paper, there was no trace of sulfate crystals in the cement paste or concrete, in spite of immersion in Na_2SO_4 solution or $MgSO_4$ solution, in spite of pure cement paste or cement + fly ash paste, in spite of under constant storage condition or sharply fluctuating storage condition. Apparently, this appearance indicates that it is very difficult that sulfate

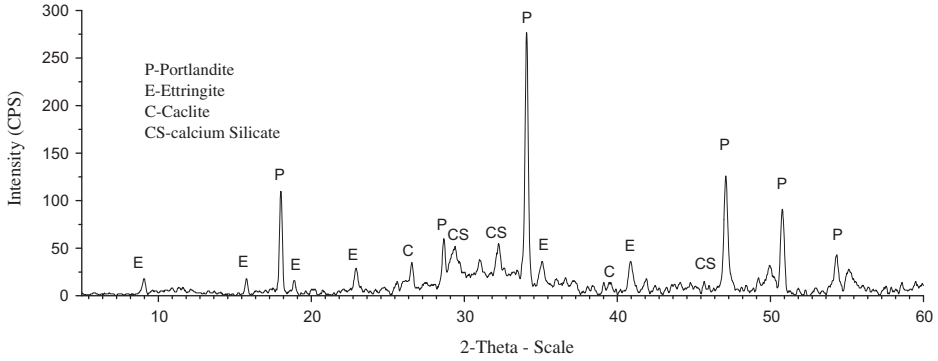

Fig. 25. XRD pattern of inner paste.

crystallization occurs in the hydrated cement paste. On the other hand, according to the observations, a large amount of ettringite, gypsum and brucite, the main chemical attack products, were detected in the cementitious materials and appeared to be responsible for the cementitious distress. This conclusion seems to be opposite to the common idea that the salt weathering process is a major cause of deterioration of concrete partially exposed to sulfate environment, however, it can logically and reasonably explain the two main controversies given in the introduction.

First, concerning the role of relative humidity in "salt weathering" on concrete. During the process of wick action higher relative humidity can result in a more widely spread high-concentration sulfate pore solution zone in partially exposed concrete, causing widespread damage by chemical sulfate attack. Lower relative humidity limits the high-concentration pore solution in a narrower zone near the surface of solution, resulting in slight deterioration.

Secondly, concerning the role of mineral additions in "salt weathering" on concrete. As we know, when the concrete is fully immersed in the sulfate solution, as pointed out by Mehta [44] for the prevention of sulfate attack "control of permeability is more important than control of the chemistry of cement", the pore size refinement due to mineral additions will prevent the sulfates to penetrate into concrete and lighten the negative effect of sulfate attack on concrete. However, in this case, during the process of wick action, the capillary rise of the solution in the concrete is given by the following equation [45]:

$$h = \frac{2\gamma_{LV} \cdot \cos\theta}{rg\rho} \tag{1}$$

where h is the height of capillary rise, γ_{LV} is the liquid/vapour interfacial energy, θ is the contact angle, r is the pore radius, g is the gravitational acceleration, and ρ is the density of solution. Just as Irassar pointed out [12], according to Eq. (1) the pore size refinement due to the mineral additions will contribute to an increase in capillary suction height. In effect, this process will draw more sulfates into the concrete, forming a severer high-concentration sulfate pore solution and causing severer chemical sulfate attack. In the paper [42], the pore solution in the cement and cement–fly ash paste was extracted by pore solution expression and the concentration of SO_4^{2-} was monitored. The results showed that the concentration of pore solution in the upper part (from the solution surface to the wet–drying interface) of cement–fly ash paste above solution is much higher than in the cement paste. For example, when pastes were partially immersed in 5% solution, after 8 weeks immersion, the SO_4^{2-} concentration of pore solution in the upper part of cement–fly ash paste is 62.62 g/l, while the concentration is 48.25 g/l in the cement paste.

On the other hand, sodium sulfate likely does not crystallize in a cement paste because in the highly alkaline pore solution other less soluble salts, e.g. ettringite, or gypsum, are preferably precipitated according to chemical equilibria theory. Salt crystallization in porous materials is difficult because salt crystallization occurrence has to reach and even exceed a threshold-supersaturation. However, the chemical reactions in pore solution can occur under any conditions and decrease the possibility of physical attack due to consuming sulfates and decreasing the sulfate concentration of pore solution. Moreover, high-concentration solution will increase the rate of chemical reaction. This will make it is very difficult that the pore solution reaches supersaturation and sodium sulfate crystallize in the cement paste even under the sharply fluctuating condition.

5. Conclusion

Researchers always attribute salt crystallization to the deterioration of concrete elements that are partially exposed to sulfate environment. However, some experimental findings are opposite to the basic mechanism of salt crystallization, both in long-term field tests or laboratory studies. Extensive micro-analysis performed on cementitious pastes partially exposed to sulfate solutions under constant and fluctuating conditions did not lead to the identification of Na_2SO_4 and $MgSO_4$ crystals On the other hand, chemical attack products such as ettringite, gypsum and brucite, were found in the weak zones. These appearances support the conclusion that the major cause for the distress of concrete partially exposed to sulfate environment is more likely to be chemical sulfate attack, not salt weathering, salt crystallization, or physical attack.

Acknowledgements

This work was financially supported by the National Science Foundation of PR China under contract #50378092, the scholarship from CSC (China Scholarship Council) and the co-funding from Ghent University of Belgium. The research was performed under a Bilateral Cooperation Agreement between Ghent University of Belgium and Central South University of PR China. The experiments were carried out at Ghent University and Central South University.

References

[1] Benavente D, García Del Cura MA, Bernabéu A, Ordóñez S. Quantification of salt weathering in porous stones using an experimental continuous partial immersion method. Eng Geol 2001;59(3–4):313–25.
[2] Folliard KJ, Sandberg P. Mechanisms of concrete deterioration by sodium sulfate crystallization durability of concrete SP-145. Farmington Hills, MI: American Concrete Institute; 1994. p. 933–45.
[3] Haynes H, O'Neill R, Mehta PK. Concrete deterioration from physical attack by salts. Concr Int 1996;18(1):63–8.

[4] Hime WG, Martinek RA, Backus LA, Marusin SL. Salt hydration distress. Concr Int 2001;23(10):43–50.
[5] Thaulow N, Sahu S. Mechanism of concrete deterioration due to salt crystallization. Mater Charact 2004;53(2–4):123–7.
[6] Yang Q, Yang Q. Effects of salt-crystallization of sodium sulfate on deterioration of concrete. J Chin Chem Soc 2007;35(7):877–80. ,885 [Chinese].
[7] Ma K, Xie Y, Long G, Liu Y. Deterioration characteristics of cement mortar by physical attack of sodium sulfate. J Chin Chem Soc 2007;35(10):1376–81.
[8] Haynes H, O'Neill R, Neff M, Mehta PK. Salt weathering distress on concrete exposed to sodium sulfate environment. ACI Mater J 2008;105(1):35–43.
[9] Mcmillan FR, Stantion TE, Tyler IL, Hansen WC. Long-time study of cement performance in concrete. Concrete exposed of sulfate soils. Portland Cement Association; 1949 (chapter 5).
[10] Stark D. Durability of concrete in sulfate-rich soils. Research and development bulletin, vol. RD O97. Portland Cement Association; 1989.
[11] Stark D. Performance of concrete in sulfate environments, RD129. Portland Cement Association; 2002.
[12] Irassar EF, Di Maio A, Batic OR. Sulfate attack on concrete with mineral admixtures. Cem Concr Res 1996;26(1):113–23.
[13] Nehdi M, Hayek M. Behavior of blended cement mortars exposed to sulfate solutions cycling in relative humidity. Cem Concr Res 2005;35(4):731–42.
[14] Rodriguez-Navarro C, Doehne E. Salt weathering: influence of evaporation rate, supersaturation and crystallization pattern. Earth Surf Process Landforms 1999;24(2–3):91–209.
[15] Haynes H, O'Neill R, Neff M, Mehta PK. Salt weathering of concrete by sodium carbonate and sodium chloride. ACI Mater J 2010;107(3):256–66.
[16] Scherer GW. Stress from crystallization of salt. Cem Concr Res 2004;34(9):1613–24.
[17] Lopez-Acevedo V, Viedma C, Gonzalez V, La Iglesia A. Salt crystallization in porous construction materials. II. Mass transport and crystallization processes. J Cryst Growth 1997;182(1–2):103–10.
[18] Gomez-Heras M, Fort R. Patterns of halite (NaCl) crystallisation in building stone conditioned by laboratory heating regimes. Environ Geol 2007;52(2):239–47.
[19] Ferraris CF, Stutzman KA. Snyder, Sulfate resistance of concrete: a new approach, research and development information PCA R&D. Serial no. 2486; 2006.
[20] Benavente D, García del Cura MA, García-Guinea J, Sánchez-Moral S, Ordóñez S. Role of pore structure in salt crystallisation in unsaturated porous stone. J Cryst Growth 2004;260(3–4):532–44.
[21] Benavente D, Martínez-Martínez J, Cueto N, García-del-Cura MA. Salt weathering in dual-porosity building dolostones. Eng Geol 2007;94(3–4):215–26.
[22] Ruiz-Agudo E, Mees F, Jacobs P, Rodriguez-Navarro C. The role of saline solution properties on porous limestone salt weathering by magnesium and sodium sulfates. Environ Geol 2007;52(2):305–17.
[23] Rodriguez-Navarro C, Doehne E, Sebastian E. How does sodium sulfate crystallize? Implications for the decay and testing of building materials. Cem Concr Res 2000;30(10):1527–34.
[24] Winkler EM, Singer PC. Crystallization pressure of salt in stone and concrete. Geol Soc Am 1972;83(11):3509–14.
[25] Tsui N, Flatt RJ, Scherer GW. Crystallization damage by sodium sulfate. J Cultural Heritage 2003;4(2):109–15.
[26] Flatt RJ. Salt damage in porous materials: how high supersaturations are generated. J Cryst Growth 2002;242(3–4):435–54.
[27] L.A. Rijniers, Salt crystallization in porous materials: an NMR study. Technische Universiteit Eindhoven; 2004.
[28] Genkinger S, Putnis A. Crystallization of sodium sulfate: supersaturation and metastable phases. Environ Geol 2007;52(2):295–303.
[29] Liu Z, De Schutter G, Deng D, Yu Z. Micro-analysis of the role of interfacial transition zone in "salt weathering" on concrete. Constr Build Mater 2010;24(11):2052–9.
[30] Cardell C, Benavente D, Rodríguez-Gordillo J. Weathering of limestone building material by mixed sulfate solutions. Characterization of stone microstructure, reaction products and decay forms. Mater Charact 2008;59(10):1371–85.
[31] Scherer GW. Factors affecting crystallization pressure. International RILEM TC 186-ISA workshop and internal sulfate attack and delayed ettringite formation, Villars, Switzerland; 2002.
[32] Scherer GW. Crystallization in pore. Cem Concr Res 1999;29(8):1347–58.
[33] Taylor HFW, Famy C, Scrivener KL. Delayed ettringite formation. Cem Concr Res 2001;31(5):683–93.
[34] Liu Z, Xiao J, Huang H, Yuan Q, Deng D. Physicochemical study on the interface zone of concrete exposed to different sulfate solutions. J Wuhan Univ Technol. (Materials Science Edition) 2006; 21(z1): 167–75.
[35] Buenfeld NR, Shurafa-Daoudi MT, Mloughlin IM. Chloride transport due to wick action in concrete, RILEM International workshop on chloride penetration into concrete; 1995. p. 315–24.
[36] Puyate YT, Lawrence CJ. Steady state solutions for chloride distribution due to wick action in concrete. Chem Eng Sci 2000;55(16):3329–34.
[37] Puyate YT, Lawrence CJ, Buenfeld NR, McLoughlin IM. Chloride transport models for wick action in concrete at large Peclet number. Phys Fluids 1998;10(3):566–75.
[38] Puyate YT, Lawrence CJ. Wick action at moderate Peclet number. Phys Fluids 1998;10(8):2114–6.
[39] Puyate YT, Lawrence CJ. Effect of solute parameters on wick action in concrete. Chem Eng Sci 1999;54(19):4257–65.
[40] Pel L, Huinink H, Kopinga K. Ion transport and crystallization in inorganic building materials as studied by nuclear magnetic resonance. Appl Phys Lett 2002;81(15):2893–5.
[41] Pel L, Huinink H, Kopinga K, Van Hees RPJ, Adan OCG. Efflorescence pathway diagram: understanding salt weathering. Build Mater 2004;18(5):309–13.
[42] Liu Z. Study of the basic mechanisms of sulfate attack on cementitious materials. Central and South University China and Ghent University Belgium; 2010.
[43] Liu Z, De Schutter G, Deng D, Liu Y. Study of cement–fly ash paste exposed to sodium sulfate solutions with different concentrations at different temperatures. In: The 2nd int. symposium on service life design for infrastructures, Delft, Netherlands, 2010.
[44] Mehta PK. Sulfate attack on concrete: a critical review, Materials science of concrete, vol. III. Amer. Ceramic Society; 1993. p. 105–30.
[45] Young JF, Mindess S, Gray RJ, Bentur A. The science and technology of civil engineering materials. Chinese Architecture & Building Press; 2006.